

A Rab10-Dependent Mechanism for Polarized Basement Membrane Secretion during Organ Morphogenesis

David W. Lerner,¹ Darcy McCoy,^{1,3} Adam J. Isabella,^{2,3} Anthony P. Mahowald,^{1,2} Gary F. Gerlach,^{1,4} Thymur A. Chaudhry,^{1,5} and Sally Horne-Badovinac^{1,2,*}

¹Department of Molecular Genetics and Cell Biology

²Committee on Development, Regeneration and Stem Cell Biology
The University of Chicago, Chicago, IL 60637, USA

³These authors contributed equally to this work

⁴Present address: Biological Sciences Graduate Program, University of Notre Dame, Notre Dame, IN 46556, USA

⁵Present address: Medical College, Rush University, Chicago, IL 60612, USA

*Correspondence: shorne@uchicago.edu

<http://dx.doi.org/10.1016/j.devcel.2012.12.005>

SUMMARY

Basement membranes (BMs) are specialized extracellular matrices that are essential for epithelial structure and morphogenesis. However, little is known about how BM proteins are delivered to the basal cell surface or how this process is regulated during development. Here, we identify a mechanism for polarized BM secretion in the *Drosophila* follicle cells. BM proteins are synthesized in a basal endoplasmic reticulum (ER) compartment from localized mRNAs and are then exported through Tango1-positive ER exit sites to basal Golgi clusters. Next, Crag targets Rab10 to structures in the basal cytoplasm, where it restricts protein delivery to the basal surface. These events occur during egg chamber elongation, a morphogenetic process that depends on follicle cell planar polarity and BM remodeling. Significantly, Tango1 and Rab10 are also planar polarized at the basal epithelial surface. We propose that the spatial control of BM production along two tissue axes promotes exocytic efficiency, BM remodeling, and organ morphogenesis.

INTRODUCTION

Basement membranes (BMs) are an ancient form of extracellular matrix found at the basal surface of all epithelia (Yurchenco, 2011). Although often overlooked as passive scaffolds, these complex protein lattices provide many essential functions to neighboring cells. In addition to providing tissue support, BMs act as signaling platforms for cell polarization, stem cell regulation, and migrating organ primordia (Arnaoutova et al., 2012; Bunt et al., 2010; Mirouse et al., 2009; O'Brien et al., 2001; Schneider et al., 2006; Wang et al., 2008). They also play central roles in organ morphogenesis and physiology (Fata et al., 2004; Miner, 2011; Miner and Yurchenco, 2004; Pastor-Pareja and Xu, 2011; Urbano et al., 2009). The misregulation of BM structure can

be a hallmark of tumor progression (Valastyan and Weinberg, 2011). Despite these critical functions, we know relatively little about the molecular control of BM assembly.

BMs are primarily composed of type IV collagen (Col IV), laminin, nidogen, and heparan sulfate proteoglycans such as perlecan or agrin. Among these components, Col IV predominates, representing up to 50% of BM proteins (Kalluri, 2003). Despite its abundance, the pathway for Col IV production is complex. Each Col IV molecule is composed of three polypeptides, two $\alpha 1$ chains and one $\alpha 2$ chain, that initiate contact at their C termini and then assemble into a triple helix, ~ 400 nm long (Khoshnoodi et al., 2008). Col IV folding requires a suite of endoplasmic reticulum (ER)-resident enzymes and chaperones, many of which are Collagen-specific (Myllyharju and Kivirikko, 2004). These proteins include lysyl- and prolyl-hydroxylase enzymes that modify the α chains both during and after translation. Special mechanisms also facilitate Col IV export. Newly synthesized proteins typically leave the ER in COPII-coated vesicles that are too small to accommodate the extended Col IV trimer (Fromme and Schekman, 2005; Jin et al., 2012; Malhotra and Erlmann, 2011). The transmembrane cargo receptor Tango1 is required at transitional ER (tER) sites to help package collagens into enlarged Golgi-bound vesicles (Saito et al., 2009; Venditti et al., 2012; Wilson et al., 2011).

Following their synthesis, new BM proteins must be targeted to the proper membrane domain for secretion. Polarized epithelial cells have distinct apical, junctional, lateral, and basal membrane domains, each of which contains a unique complement of lipids and proteins. These domains are established and maintained by polarized vesicle traffic that delivers newly synthesized secreted and transmembrane proteins to the appropriate cell surface (Mellman and Nelson, 2008; Rodriguez-Boulan et al., 2005). Although much is known about the trafficking pathways that target transmembrane proteins to the combined basal and lateral surfaces, there have long been indications that BM proteins reach the basal surface through a distinct mechanism (Boll et al., 1991; Caplan et al., 1987; Cohen et al., 2001; De Almeida and Stow, 1991). The first molecular evidence for this assertion came from genetic studies in *Drosophila* that identified the DENN domain protein, Crag, and the protease-like protein, Scarface (Scaf), as selective regulators

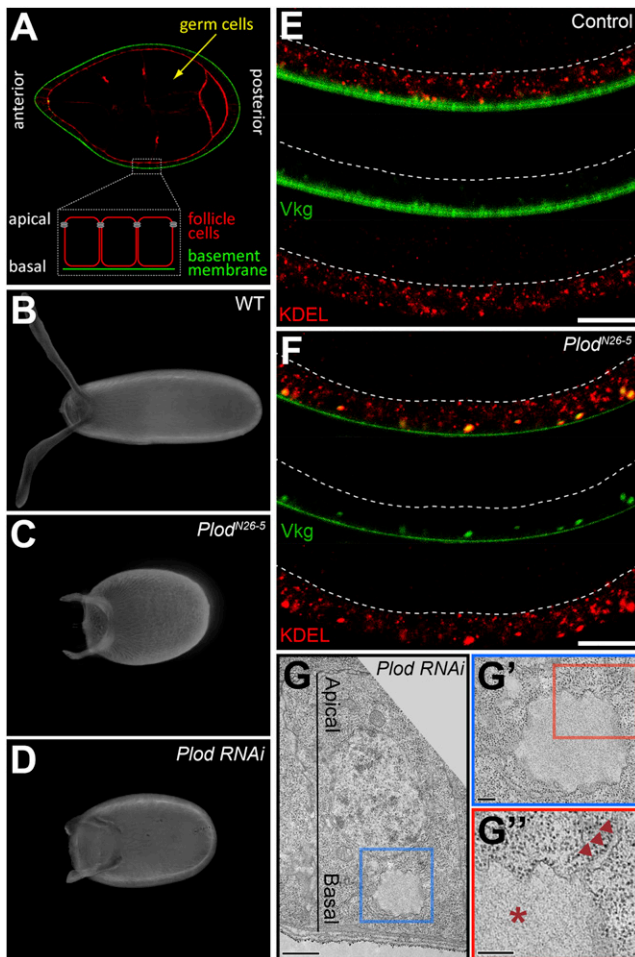


Figure 1. *Plod*^{N26-5} Disrupts the Secretion of Col IV
 (A) Overview of egg chamber structure at stage 8. Actin (red), Vkg-GFP (green).
 (B–D) Representative egg shapes for wild-type (B), *Plod*^{N26-5} (C), and *Plod*-RNAi (D).
 (E) In wild-type, proteins with the KDEL ER retention signal are throughout the cell, whereas Vkg-GFP is in the BM. Dashed lines mark the apical surface. Scale bar represents 10 μ m. Experiments performed at stages 7–8.
 (F) In *Plod*^{N26-5}, Vkg-GFP punctae overlap with KDEL near the basal surface, indicating ER accumulation. Dashed lines mark the apical surface. Scale bar represents 10 μ m. Experiments performed at stages 7–8.
 (G) TEM of a single *Plod*-RNAi follicle cell showing a distended ER region in the basal cytoplasm. Scale bar represents 1 μ m. Experiments performed at stages 7–8.
 (G' and G'') Magnifications of the image in (G). Ribosomes decorate the distended ER cisterna (asterisk) and adjacent, normal ER membranes (arrowheads). Scale bars represent 200 nm.
 See also Figure S1.

of polarized BM deposition (Denef et al., 2008; Eastburn and Mostov, 2010; Sorrosal et al., 2010). Loss of either gene causes BM proteins to accumulate on both the basal and apical epithelial surfaces without obvious effects on other exocytic cargo. Currently, the mechanisms by which Crag and Scaf promote polarized BM secretion are unknown.

The *Drosophila* egg chamber provides a highly tractable system for the study of BM biology in the context of a developing

organ. Egg chambers are multicellular structures within fly ovaries that will each give rise to a single egg. They are composed of an inner germ cell cluster surrounded by an outer epithelial layer of follicle cells. The apical follicle cell surfaces face the germ cells, whereas the basal surfaces contact the BM (Figure 1A). The BM, in turn, forms the egg chamber's outer most layer. To our knowledge, the follicle cells are the only fly epithelium that synthesizes all major BM components (Mirre et al., 1988; Pastor-Pareja and Xu, 2011; Yasothornsrikul et al., 1997).

Interestingly, the follicle cell BM plays a critical role in shaping the fly egg. Though initially spherical, egg chambers lengthen along their anterior-posterior (AP) axes as they develop. This morphogenesis depends on an unusual form of planar polarity, in which actin filaments at the basal cell surface become aligned orthogonal to the AP axis (Gutzeit, 1990). Once oriented, the follicle cells undergo a directed migration along the inner BM surface, a process that causes the entire egg chamber to rotate inside the stationary matrix (Haigo and Bilder, 2011). Importantly, the migrating follicle cells also secrete new BM proteins. Through a process that is still poorly understood, the combination of cell movement and matrix secretion creates fibril-like structures in the BM, perpendicular to the elongation axis (Gutzeit et al., 1991; Haigo and Bilder, 2011; Schneider et al., 2006) (Figure S1A available online). It has been proposed that this fibrillar matrix then constrains isometric egg chamber growth to promote AP elongation, but many questions remain about how this unusual BM structure is built.

Here, we identify a mechanism for polarized BM secretion in the follicle cells. Starting from a mutation that traps Col IV in the cell, we show that BM proteins are locally synthesized in a basal ER compartment, and are exported through Tango1-positive ER exit sites to basal Golgi clusters. We then introduce Rab10 as a regulator of polarized BM secretion, and show that Crag regulates Rab10 in this context. Finally, we show that the BM exocytic machinery is also planar polarized at the basal epithelial surface. Our data suggest that BM proteins are secreted from the trailing edge of each migrating follicle cell, a process that may contribute to the formation of BM fibrils and egg chamber elongation. We therefore propose that the spatial regulation of BM production along two tissues axes promotes both polarized secretion and matrix remodeling during organ morphogenesis.

RESULTS

Col IV Accumulates in a Basal ER Region in *Plod* Mutant Follicle Cells

We have previously reported a genetic screen for mutations that block egg chamber elongation and produce round eggs (Horne-Badovinac et al., 2012). The RE-H complementation group from this screen contained a single allele, *N26-5* (Figures 1B and 1C). We used deficiency mapping to localize *N26-5* to a chromosomal region containing the *procollagen lysyl hydroxylase* (*Plod*) gene. Sequencing the *Plod* coding regions in *N26-5* mutant larvae identified a lesion, which is predicted to change a highly conserved glycine to aspartic acid in one of the protein's catalytic domains (Figure S1B). RNAi knockdown of *Plod* in the

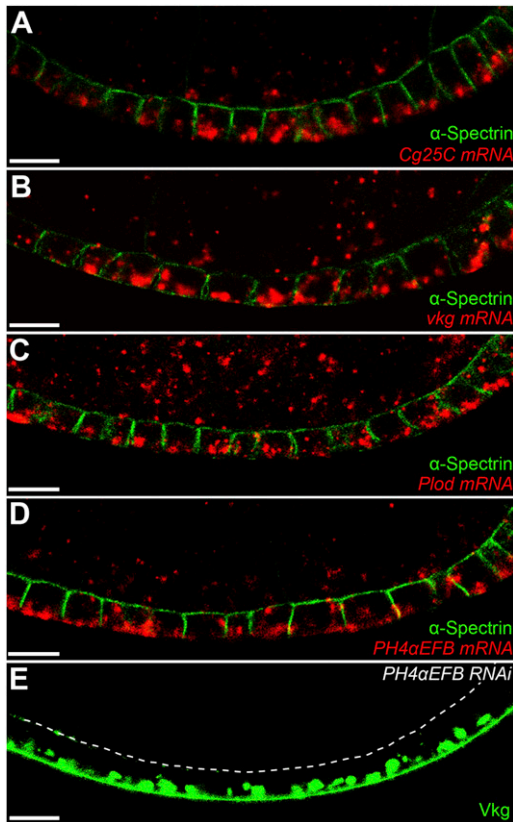


Figure 2. Col IV Is Synthesized in the Basal ER

(A–D) mRNAs encoding the Col IV α chains Cg25C (A) and Vkg (B), and the Col IV biosynthetic enzymes Plod (C) and PH4 α EFB (D) are all enriched in the basal cytoplasm. α -Spectrin marks the apical and lateral epithelial surfaces. (E) *PH4 α EFB-RNAi* causes Vkg-GFP to accumulate in the basal ER. The dashed line marks the apical surface. Experiments performed at stages 7–8. Scale bars represent 10 μ m. See also Figure S2.

follicle cells also produces round eggs (Figure 1D). We now refer to this mutation as *Plod*^{N26-5}.

Plod is an ER-resident enzyme that co- and posttranslationally modifies lysine residues on Col IV α chains (Myllylä et al., 2007). Previous work in *Drosophila* and other organisms has shown that Plod depletion leads to Col IV retention in the ER (Bunt et al., 2011; Norman and Moerman, 2000; Rautavuoma et al., 2004; Schneider and Granato, 2006; Sipilä et al., 2007). *Drosophila* have only one Col IV isoform, in which the α 1 and α 2 chains are Collagen gene at 25C (Cg25C) and Viking (Vkg), respectively (Natzle et al., 1982; Yasothornsrikul et al., 1997). To determine whether Col IV is retained in the ER of *Plod*^{N26-5} cells, we used a GFP protein trap in the *vkg* locus (Vkg-GFP) (Buszczak et al., 2007). When wild-type follicle cells are viewed along their apical-basal axes, Vkg-GFP is typically only visible within the BM (Figure 1E). As expected, *Plod*^{N26-5} follicle cells show intracellular Vkg-GFP accumulation, as well as reduced Vkg-GFP in the BM. However, we were surprised to find that the intracellular Col IV is always located near the basal surface, whereas the distribution of KDEL ER-retention signal and the ER membrane dye ER-tracker both reveal that this organelle extends

throughout the cytoplasm (Figures 1E, 1F, S1C, and S1D). By performing transmission electron microscopy (TEM) on follicle cells expressing *Plod-RNAi*, we found that the ER structure is normal except for unusually distended basal ER cisternae, where the Col IV is presumably trapped (Figure 1G). These data indicate that Col IV accumulates in a basal ER compartment in *Plod*-depleted cells.

BM Proteins Are Locally Synthesized in a Basal ER Compartment

The pattern of Col IV accumulation in *Plod*^{N26-5} cells led us to hypothesize that Col IV may be synthesized near the basal surface. Indeed, \sim 70% of *Cg25C* and *vkg* mRNAs localize to the basal half of the cytoplasm, making it likely that the Col IV α chains are translated directly into the basal ER (Figures 2A, 2B, and S2A). Col IV protein is also basally enriched in wild-type cells (Figures S2B and S2C). Plod and Prolyl-4-hydroxylase- α EFB (PH4 α EFB) enzymes modify Col IV α chains as they are translocated across the ER membrane (Myllyharju and Kivirikko, 2004). Significantly, the mRNAs for these proteins show a similar localization (Figures 2C, 2D, and S2A). Moreover, *PH4 α EFB-RNAi* causes Col IV to become trapped in the basal ER, similar to loss of Plod (Figures 2E and S2D). Basal enrichment is not a general property of follicle cell mRNAs, as we and others have also identified ER-associated transcripts that localize to the apical cytoplasm (Home-Badovinac and Bilder, 2008; Konsolaki and Schüpbach, 1998; Li et al., 2008). Together, these data indicate that Col IV is predominantly synthesized in a basal ER compartment in wild-type follicle cells.

Col IV production in the basal ER raises the possibility that local synthesis promotes polarized secretion to the BM. Unlike mammalian cells in which the Golgi often forms a singular organelle called the Golgi ribbon, *Drosophila* cells have a distributed system in which small Golgi clusters are found throughout the cytoplasm. Each cluster is associated with a transitional ER (tER) site, from which newly synthesized proteins exit the ER. This organization of the early secretory pathway makes it possible for proteins synthesized in a subregion of the ER to be dispatched through the tER-Golgi units closest to the targeted plasma membrane (Kondylis et al., 2009; Kondylis and Rabouille, 2009).

To determine whether Col IV exits the ER from the basal region where it is synthesized, we investigated the function of the Tango1 cargo receptor, which helps package Col IV into enlarged Golgi-bound vesicles (Saito et al., 2009; Wilson et al., 2011). For these studies, we raised an antibody against Tango1 and validated its specificity (Figure S3A). This protein localizes to \sim 90% of tER-Golgi units, as shown by colocalization with the CopII-associated GTPase Sar1 and the *cis*-Golgi marker GM130 (Figures 3A, S3B, and S3C). Although tER-Golgi units are evenly distributed along the apical-basal axis, the Tango1 signal is much stronger at basal tER sites (Figures 3A, S3B, and S3D). Significantly, Vkg-GFP also accumulates at the basal Tango1-positive tER sites in wild-type cells (Figure 3B), and *Tango1-RNAi* causes most Vkg-GFP to become trapped in the basal ER (Figures 3C and S3E). It therefore appears that most Col IV exits the ER through basally-localized tER-Golgi units.

We next asked whether other BM proteins are also synthesized in the basal ER. Quantification of intracellular laminin and

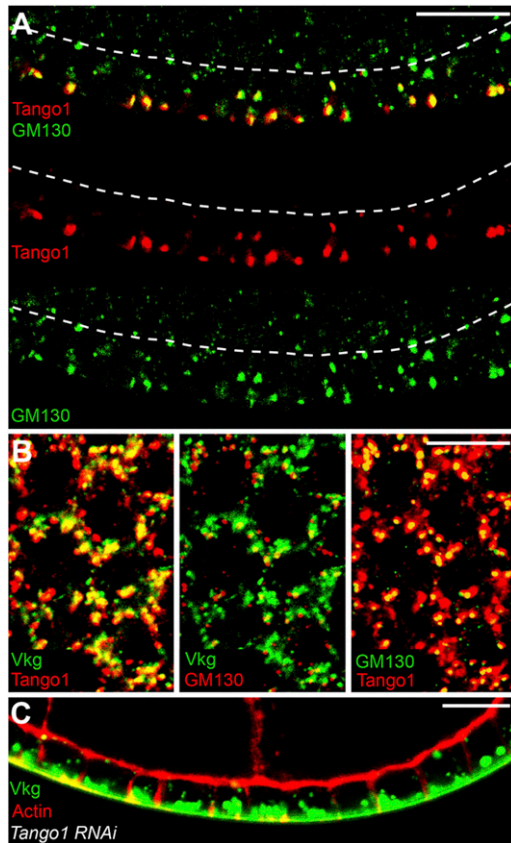


Figure 3. Tango1 Mediates Col IV ER Exit Predominantly at Basal tER Sites

(A) Tango1 is strongly enriched at basal tER-Golgi units, as indicated by the *cis*-Golgi marker, GM130. Dashed lines mark the apical surface. (B) An optical section through the basal cytoplasm showing colocalization between Tango1, GM130, and Vkg-GFP. (C) *Tango1-RNAi* causes Vkg-GFP to accumulate in the basal ER. Experiments performed at stages 7–8. Scale bars represent 10 μ m. See also Figure S3.

perlecan (Trol in *Drosophila*) levels revealed that these proteins are also enriched in the basal cytoplasm (Figures S4A–S4D). Moreover, *Tango1-RNAi* causes both proteins to accumulate in the basal ER with Col IV (Figures 4A and 4B). To investigate whether these proteins are translated directly into the basal ER, we again examined mRNA localization. Similar to the Col IV-encoding mRNAs, *Laminin B1* transcripts are enriched in the basal cytoplasm (Figures 4C and S4E). Conversely, *trol* transcripts show no basal bias (Figures 4D and S4E), suggesting that this protein's enrichment in the basal ER occurs by a separate mechanism. These data suggest that Laminin is also synthesized in the basal ER, and that other BM proteins may exit with Col IV through Tango1-positive tER sites.

Crag Regulates Rab10 to Promote Polarized BM Secretion

If BM proteins predominantly traffic through basal tER-Golgi units, how then do they reach the basal cell surface? Rab proteins are small GTPases that function as master regulators

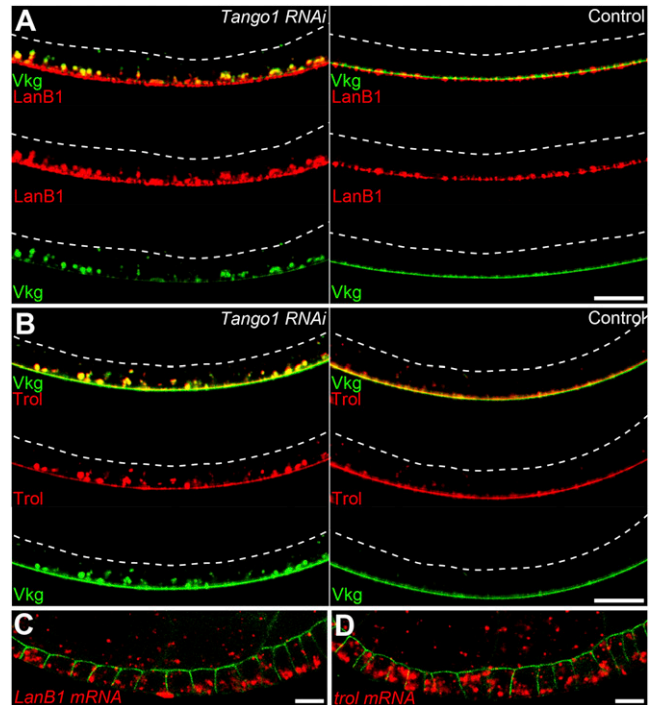


Figure 4. Laminin and Trol Are Also Enriched in the Basal Cytoplasm (A and B) *Tango1-RNAi* causes LanB1 (A) and Trol (B) to accumulate in the basal ER with Vkg-GFP. Dashed lines mark the apical surface. (C) *LanB1* mRNA is basally enriched. α -Spectrin marks the apical and lateral epithelial surfaces. (D) *trol* mRNA does not show a basal bias. α -Spectrin marks the apical and lateral epithelial surfaces. Experiments performed at stages 7–8. Scale bars represent 10 μ m. See also Figure S4.

of intracellular membrane traffic (Hutagalung and Novick, 2011). Using a transgenic collection of YFP-tagged Rabs (Zhang et al., 2007), we found that Rab10 has an intriguing localization pattern. In addition to general cytoplasmic staining, there is a strong YFP-Rab10 signal near the basal follicle cell surface (Figures 5A and S5A). Significantly, *Rab10-RNAi* causes large BM proteins like Col IV, perlecan and laminin to accumulate on both the basal and apical surfaces (Figures 5B–5D); this phenotype is seen to a lesser extent with the smaller BM protein nidogen (Figure S5B). In contrast, *Rab10-RNAi* has no effect on the localization of four other proteins that normally undergo polarized trafficking in the follicle cells (Figures 5E, 5G, and S5C). The basal enrichment of BM-encoding mRNAs and Tango1 is also normal under these conditions (Figures S5D–S5F). Thus, Rab10 is required downstream of the basal bias in BM synthesis to ensure that BM proteins are delivered exclusively to the basal cell surface.

The apical accumulation of BM proteins in Rab10-depleted cells is remarkably similar to the phenotype first described for *Crag* (Denef et al., 2008). We therefore investigated the relationship between these two proteins. Although *Crag* is broadly distributed along the follicle cell apical-basal axis (Denef et al., 2008), an optical section near the basal surface revealed that *Crag* and Rab10 colocalize in this region (Figures 6A and S6A).

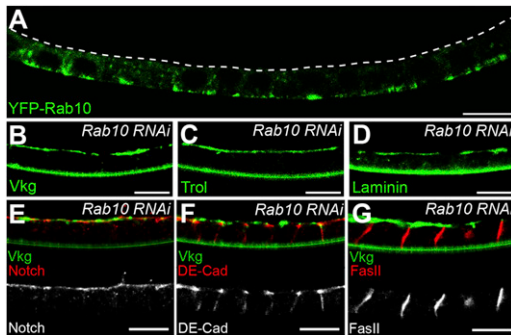


Figure 5. Rab10 Promotes Polarized BM Secretion

(A) YFP-Rab10 is enriched near the basal follicle cell surface. The dashed line marks the apical surface. (B–D) *Rab10-RNAi* mis-targets Col IV (Vkg-GFP) (B), Perlecan (Trol-GFP) (C), and laminin to the apical surface (D). (E–G) *Rab10-RNAi* does not affect the localization of apical (Notch) (E), junctional (DE-Cadherin) (F), or lateral (FasII) transmembrane proteins (G). Rab10 knockdown is shown by apical Vkg-GFP. Experiments performed at stages 7–8, except (C) and (D), which are stage 9. Scale bars represent 10 μ m. See also Figure S5.

Moreover, in *Crag^{GG43}* follicle cell clones, the strong YFP-Rab10 signal largely disappears from the basal surface, and is redistributed to the apical cytoplasm (Figures 6B and S6B). *Rab10* mRNA shows a 60% basal enrichment, which is unchanged under *Crag-RNAi* (Figure S6C). It therefore appears that *Crag* is required for the posttranslational targeting of Rab10 to structures near the basal cell surface.

Recently, *Crag*'s mammalian homologs have been shown to function as highly specific Rab10 guanine nucleotide exchange factors (GEFs) in vitro (Yoshimura et al., 2010). Rab proteins with mutations that block GTP binding are thought to act as dominant negatives, in part, by sequestering GEFs (Li and Stahl, 1993; Stenmark et al., 1994). If *Crag* is a Rab10 GEF in this system, overexpressing *Crag* together with a Rab10.T23N dominant negative transgene may suppress the dominant negative phenotype (Zhu et al., 2007). Similar to *Rab10-RNAi*, expression of *UAS-Rab10.T23N* causes Vkg-GFP to accumulate on the apical surface (Figure 6E). Importantly, coexpressing *UAS-HA-Crag* with *UAS-Rab10.T23N* rescues this defect (Figures 6C–6F). We have also confirmed that *Crag* and Rab10 physically interact through coimmunoprecipitation experiments (Figure S6D). Combined with the mammalian data, these results argue that *Crag* functions as a Rab10 GEF to promote polarized BM secretion.

Denn domain proteins can bind multiple Rabs through interactions both within and outside their GEF domain. *Crag* has been previously shown to colocalize with Rab5 and Rab11 in the follicle cells (Denef et al., 2008). Rab5 depletion has no effect on polarized BM secretion (Figure S6E). Interestingly, however, we did observe Rab11 punctae interspersed with the *Crag* and Rab10 signals in the basal cytoplasm (Figure S6F). To investigate whether Rab11 regulates BM secretion, we followed Vkg-GFP localization under a series of RNAi conditions. Unlike the situation with *Rab10-RNAi* (Figures 5B and 6I), the Vkg-GFP localization in Rab11-depleted cells is similar to wild-type controls (Figures 6G and 6H). However, when we simultaneously

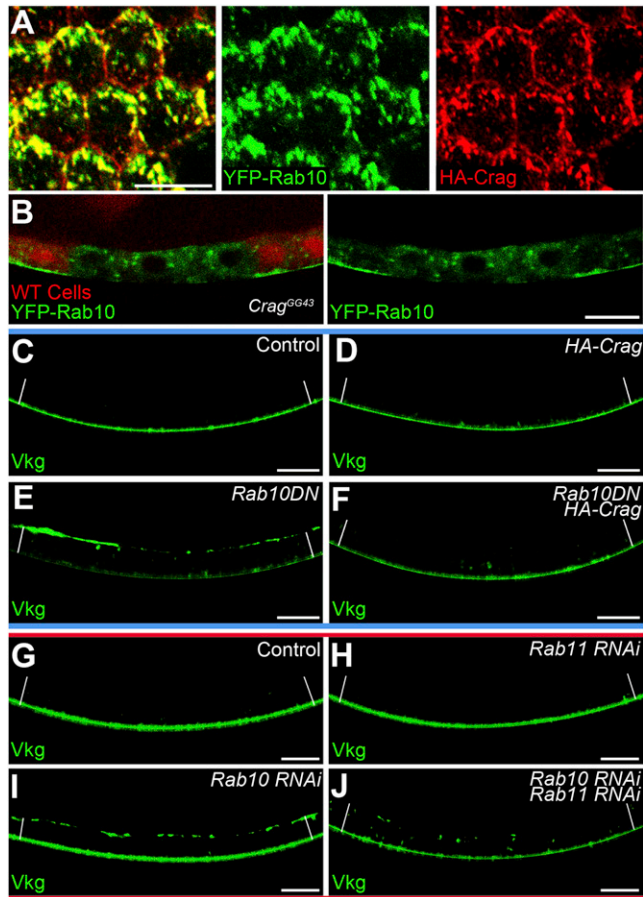


Figure 6. Crag Regulates Rab10 during Polarized BM Secretion

(A) Optical section near the basal surface showing YFP-Rab10 and HA-Crag colocalization. (B) A *Crag^{GG43}* follicle cell clone shows a redistribution of YFP-Rab10 away from the basal surface. (C and D) Interaction between *UAS-HA-Crag* and *UAS-Rab10.T23N*. Vkg-GFP localization is normal in wild-type (C) and *UAS-HA-Crag* (D) follicle cells. White lines extend between the apical and basal epithelial surfaces. (E) Interaction between *UAS-HA-Crag* and *UAS-Rab10.T23N*. A *UAS-Rab10.T23N* dominant negative transgene causes Vkg-GFP to accumulate on the apical surface. A YFP on Rab10.T23N contributes to the fluorescent signal in the cytoplasm. White lines extend between the apical and basal epithelial surfaces. (F) Interaction between *UAS-HA-Crag* and *UAS-Rab10.T23N*. Coexpression of *UAS-HA-Crag* with *UAS-Rab10.T23N* suppresses this phenotype. A YFP on Rab10.T23N contributes to the fluorescent signal in the cytoplasm. White lines extend between the apical and basal epithelial surfaces. (G and H) Interaction between *Rab10-RNAi* and *Rab11-RNAi*. Vkg-GFP localization is normal in (G) wild-type and (H) Rab11-depleted cells. White lines extend between the apical and basal epithelial surfaces. (I) Interaction between *Rab10-RNAi* and *Rab11-RNAi*. Rab10 depletion causes Vkg-GFP to accumulate on the apical surface. White lines extend between the apical and basal epithelial surfaces. (J) Interaction between *Rab10-RNAi* and *Rab11-RNAi*. Codepletion of Rab10 and Rab11 eliminates the apical Vkg-GFP and increases the cytoplasmic signal. White lines extend between the apical and basal epithelial surfaces. Experiments performed at stages 7–8. Scale bar represents 10 μ m. See also Figure S6.

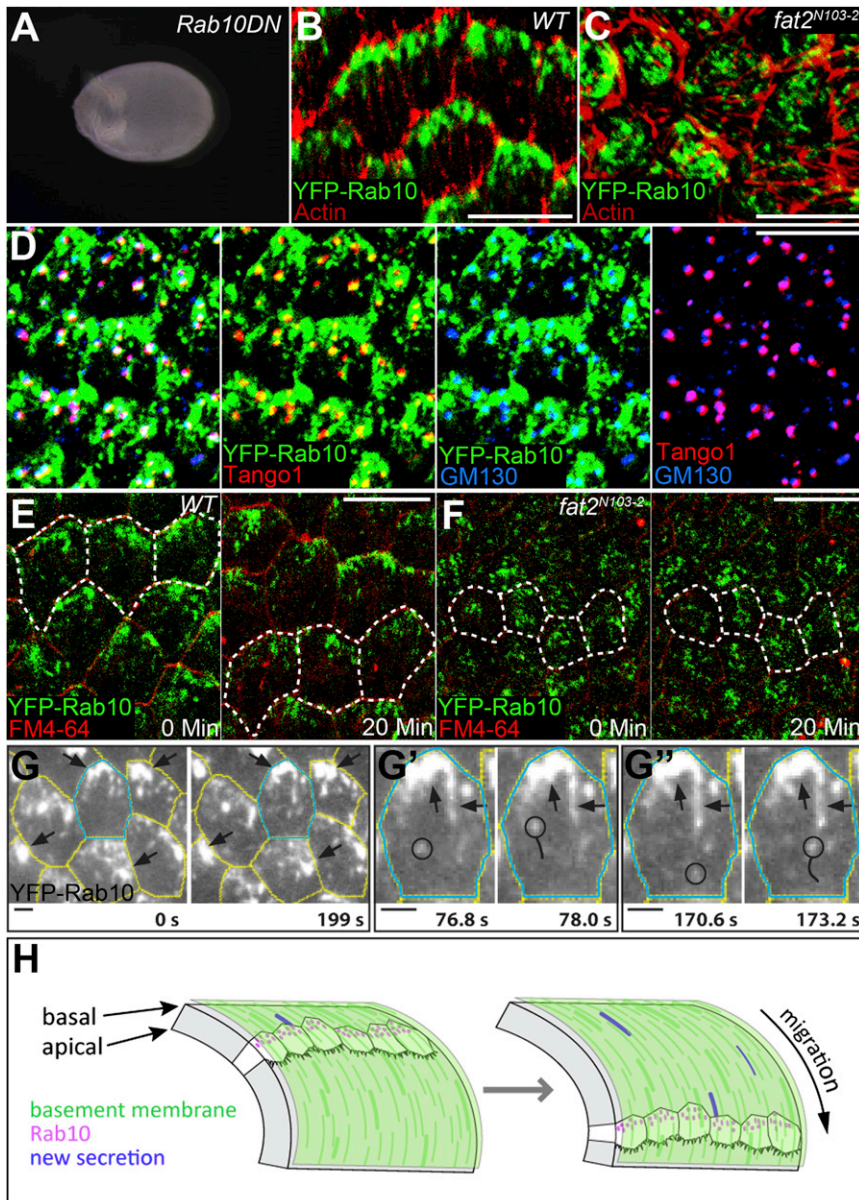


Figure 7. The BM Exocytic Machinery Is Planar Polarized at the Basal Epithelial Surface

(A) Rab10.T23N expression produces round eggs. (B) YFP-Rab10 is planar polarized at the level of the basal actin filaments. Scale bar represents 10 μ m. (C) YFP-Rab10's planar polarization is lost in *fat2^{N103-2}* epithelia. Scale bar represents 10 μ m. (D) Tango1 and GM130 are also planar polarized and partially overlap with YFP-Rab10. Scale bar represents 10 μ m. (E) Live imaging reveals that YFP-Rab10 is enriched at the trailing edge of each migrating cell. Scale bar represents 10 μ m. FM4-64 marks cell membranes. Dashed lines mark the same three to four cells at each time point. (F) *fat2^{N103-2}* epithelia fail to migrate and YFP-Rab10 is mispolarized. Scale bar represents 10 μ m. FM4-64 marks cell membranes. Dashed lines mark the same three to four cells at each time point. (G-G'') TIRF microscopy reveals that larger Rab10-positive structures are largely immobile (arrows), whereas smaller Rab10-positive structures (circles in G' and G'') move rapidly through the cytoplasm. Scale bars represent 2 μ m. (H) Speculative model for how planar polarization of BM secretion would synergize with follicle cell migration to create the unusual BM fibrils associated with egg chamber elongation. Illustration adapted from Bilder and Haigo (2012). Experiments performed at stages 7–8. See also Figure S7 and Movies S1, S2, and S3.

depleted Rab10 and Rab11, Vkg-GFP was no longer found on the apical surface, but often showed a punctate intracellular distribution, in addition to its BM localization (Figure 6J). This phenotype was also observed with simultaneous depletion of Crag and Rab11 (Figures S6G–S6J). We conclude that Rab11 does not regulate BM secretion under normal conditions, but that in the absence of Crag or Rab10, BM proteins are inappropriately targeted to the apical surface through a Rab11-dependent mechanism.

Planar Polarization of the BM Exocytic Machinery during Egg Chamber Elongation

All experiments described above were performed during oogenic stages 6–8, which is the peak period of Col IV production in the egg chamber (Haigo and Bilder, 2011). Significantly, this is also the time when planar polarization of the follicle

cell epithelium first drives egg chamber elongation. We noticed that Rab10.T23N expression in the follicle cells produces round eggs (Figure 7A). Moreover, YFP-Rab10 shows a striking planar polarization at the basal epithelial surface, when viewed at the basal actin filaments (Figure 7B). Tango1, GM130, and the translocon protein Sec61 α are also planar polarized (Figures 7D, S7A, and S7B). Consistent with Rab10's role in mediating late stages of protein traffic to the plasma membrane (Cao et al., 2008; Chen et al., 2012; Sano et al., 2007; Schuck et al., 2007), most of the YFP-Rab10 signal lies between the Tango1-positive tER-Golgi units and a basal region of the lateral plasma membrane (compare Figure 7D with 7B and 7E). Rab10 also partially overlaps with the tER-Golgi units (Figure 7D), but is not required for their planar polarization (Figure S7B). This unexpected positioning of the BM exocytic machinery suggests that BM deposition may be polarized along both the apical-basal and planar axes during egg chamber elongation.

How does Rab10 become localized along the planar axis? The atypical cadherin Fat2 is a key regulator of follicle cell planar polarity (Viktorinová et al., 2009). In *fat2^{N103-2}* epithelia, YFP-Rab10 is polarized normally along the apical-basal axis,

but is mislocalized within the epithelial plane (Figures 7C, S7C, and S7D). This effect is posttranslational, as *Rab10* mRNA is not polarized along the planar axis (Figure S7E). Interestingly, this pattern is the opposite of *Crag* loss of function, where *Rab10*'s apical-basal polarization is disrupted, but the protein still present at the basal surface is planar polarized (Figures 6B, S6B, and S7F). Thus, *Rab10*'s polarization along the apical-basal and planar axes is controlled by two different mechanisms, one requiring *Crag* and the other requiring *Fat2*.

Follicle cell planar polarity is intimately linked with a directed epithelial migration that creates fibril-like structures in the BM. Live imaging of wild-type epithelia revealed that the intense YFP-*Rab10* signal corresponds to the trailing edge of each migrating cell (Figure 7E; Movie S1). Conversely, *fat2*^{N703-2} epithelia do not migrate, and BM structure is highly disrupted (Figures 7F and S7G; Movie S2). Near-total internal reflection fluorescence (TIRF) imaging (Konopka and Bednarek, 2008; Tokunaga et al., 2008) of wild-type cells at higher temporal resolution shows that the large, *Rab10*-positive structures at the trailing edge are surprisingly stable (on the order of minutes), whereas smaller *Rab10*-positive structures move at speeds of up to 1 $\mu\text{m/s}$ through the basal cytoplasm (Figure 7G; Movie S3). Although we do not yet know the identity of these *Rab10*-positive compartments, these observations suggest that newly synthesized BM proteins are secreted from the trailing edge of each follicle cell as it migrates, which may have important implications for BM remodeling during elongation morphogenesis.

DISCUSSION

The BM is essential for epithelial structure and morphogenesis; yet little is known about how the component proteins are secreted to the basal surface, or how this process is regulated during development. Here, we have shown that the synthesis and trafficking of BM proteins is largely restricted to the basal cytoplasm in the *Drosophila* follicle cells. We have also identified *Rab10* as a key regulator of polarized BM secretion, and shown that *Crag* likely functions as a *Rab10* GEF. Surprisingly, the BM exocytic machinery shows a striking planar polarity at the basal epithelial surface, specifically during the time when the BM is being remodeled to promote egg chamber elongation. We therefore propose that spatial control of BM production along two tissue axes may promote exocytic efficiency, BM remodeling, and organ morphogenesis.

The polarized deposition of the two major BM components, Col IV and laminin, appears to begin with the targeting of their transcripts to the basal cytoplasm. For mRNA localization to enhance polarized membrane traffic requires that the cell have distributed tER-Golgi units, as opposed to a single Golgi ribbon (Kondylis et al., 2009; Kondylis and Rabouille, 2009). With this modular organization, localized mRNAs can be translated into a subregion of the ER, and newly synthesized proteins quickly dispatched through the tER-Golgi units closest to the target cell surface. Elegant studies in *Drosophila* have documented the use of this strategy for the polarized secretion of the TGF α homolog Gurken in the oocyte, and for the apical secretion of Wingless in the embryo (Herpers and Rabouille, 2004; Simmonds et al., 2001). Moreover, the targeting of mRNAs

encoding secreted and transmembrane proteins to neuronal dendrites containing Golgi outposts (structures analogous to tER-Golgi units) suggests that this distributed exocytic program is conserved in at least some vertebrate cells (Ramírez and Couve, 2011). We propose that the basal targeting of the Col IV- and laminin-encoding mRNAs may similarly enhance the delivery of these proteins to the basal surface.

The local synthesis of BM components may also address several challenges that these complex proteins pose to the ER. For example, Col IV requires dedicated machinery to mediate both trimer formation and ER exit. Concentrating these functions into a smaller ER region is therefore likely to increase Col IV biosynthetic efficiency. We have shown that the mRNAs encoding Plod and PH4 α EFB are also enriched in the basal cytoplasm, and that loss of either protein causes Col IV to accumulate in the basal ER. Tango1 function is also higher at basal ER exit sites. Interestingly, the ECM component Aggrecan is synthesized in a restricted ER region in avian chondrocytes (Vertel et al., 1989). Thus, ER compartmentalization may be a conserved strategy for ECM biosynthesis.

Although local synthesis likely facilitates polarized BM secretion, additional downstream mechanisms are required to restrict protein delivery to the basal surface. The first evidence for this regulation came from Deneff et al. (2008), who showed that loss of *Crag* causes BM proteins to accumulate on both the basal and apical follicle cell surfaces. The presence of the DENN domain made it likely that *Crag* was a direct regulator of polarized membrane traffic. Consistent with this notion, *Crag* localized to *Rab5*- and *Rab11*-positive endosomes, and along the apical and lateral plasma membranes (Deneff et al., 2008). However, the diversity of the protein's distribution made it difficult to pinpoint *Crag*'s function in polarized BM secretion.

Here, we have identified *Rab10* as a second critical component in this system. Importantly, this protein shows a more restricted localization, with the strongest *Rab10* signal being tightly associated with the basal cell surface. *Crag* colocalizes with *Rab10* in this region and is required for *Rab10*'s basal enrichment. Moreover, *Rab10* interacts with *Crag* both genetically and physically, and *Rab10* depletion phenocopies *Crag*'s BM defect. Given that *Crag*'s mammalian homologs function as *Rab10* GEFs in vitro (Yoshimura et al., 2010), we now propose that *Crag* functions as a *Rab10* GEF in vivo to control polarized BM secretion.

It is likely, however, that *Crag* also has *Rab10*-independent functions. For instance, *Crag* mutant cells show defects in apical-basal polarity (Deneff et al., 2008), whereas *Rab10*-depleted cells do not (data not shown). This phenotypic difference could be due to incomplete *Rab10* knockdown, but it is also consistent with *Crag* regulating more than one trafficking pathway. DENN domain proteins can bind multiple Rabs through interactions outside their GEF domain (Marat et al., 2011). Because *Crag* also colocalizes with *Rab5* and *Rab11*, both of which are required for follicle cell apical-basal polarity (Lu and Bilder, 2005; Xu et al., 2011), *Crag* may play a second role with these proteins controlling epithelial architecture.

How then does *Rab10* control polarized BM secretion? We have shown that *Rab10* has a complex distribution in the basal cytoplasm, where it associates both with Tango1-positive tER-Golgi units and the plasma membrane. *Rab10* is a known

exocytic regulator in multiple organisms and cell types; however, the exact compartment(s) to which it localizes vary with cargo and cell polarization state (Babbey et al., 2006, 2010; Chen et al., 2006; Sano et al., 2007; Schuck et al., 2007; Wang et al., 2011). A recent proteomic analysis in MDCK cells found Rab10 on exocytic vesicles bound for a basal region of the lateral plasma membrane (Cao et al., 2008). We propose that Rab10 may localize to similarly targeted exocytic vesicles in the follicle cells. Interestingly, Rab10 is not absolutely required for basal secretion, as a significant fraction of BM proteins do reach the basal surface when Rab10 is depleted. However, it is required to stop BM proteins from taking an alternate, Rab11-dependent route to the apical surface. Thus, local synthesis may provide sufficient information for the basal targeting of some BM vesicles, but Rab10 is required to ensure robust polarized secretion.

In addition to identifying mechanisms directing BM secretion to the basal surface, this work also provides a strong foundation for future studies of BM remodeling during egg chamber elongation. We have shown that the BM exocytic machinery is enriched at the trailing edge of each migrating follicle cell in a Fat2-dependent manner, a surprising observation given that many migrating cells orient their Golgi toward the front (Sütterlin and Colanzi, 2010; Yadav and Linstedt, 2011). It has been proposed, however, that the entire purpose of follicle cell migration is to create the unusual fibril-like structures in the BM that promote egg chamber elongation (Haigo and Bilder, 2011). We have not yet identified the exact location where BM proteins exit the cell; however, Rab10's known function as a late exocytic regulator evokes the following model. We envision that newly synthesized BM proteins are quickly transported from basal tER-Golgi units to the trailing plasma membrane through a Rab10-dependent mechanism. Planar polarized secretion then synergizes with cell movement to produce the fibril-like structures in the BM (Figure 7H). Whether Rab10 directly regulates planar secretion is not yet clear, as the BM material that reaches the basal surface under Rab10 depletion still shows the fibril-like morphology (data not shown). However, incomplete depletion and/or partial redundancy with closely related Rabs may obscure this aspect of Rab10's function (Schuck et al., 2007; Shi et al., 2010). The follicle cells thus provide a powerful system to investigate the dynamic regulation of BM secretion and remodeling during organ morphogenesis.

EXPERIMENTAL PROCEDURES

Drosophila Genetics

Follicle cell clones were generated using *e22c-Gal4* to drive expression of the FLP recombinase. UAS transgenes were expressed with *TubP-Gal4* or *traffic jam-Gal4* (*tj-Gal4*) for full follicle cell expression, or *hs-FLP*; *Act5c* >> *Gal4* for clones. Most lines are from the Bloomington *Drosophila* stock center, with exceptions listed below. RNAi lines for Plod, Tango1, and Rab5 are from the Vienna *Drosophila* RNAi Center. *Rab11-RNAi* is from Satoh et al. (2005). *tj-Gal4* (NP1624) is from the *Drosophila* Genetic Resource Center, Kyoto. *vkg-GFP* (CC00791), *trtl-GFP* (CA06698), *Sar1-GFP* (CA07674), and *Sec61 α -GFP* (CC00735) are from Buszczak et al. (2007). *Crag^{GG43}*, *FRT19A*, and *UAS-HA-Crag* are from Deneff et al. (2008). *fat2^{N103-2}*, *FRT80* is from Horne-Badovinac et al. (2012). *w¹¹¹⁸* typically served as a wild-type control. Most crosses were raised, and experiments performed at 25°C. Full genotypes for each experiment and unusual temperature conditions can be found in Supplemental Experimental Procedures.

Fluorescent In Situ Hybridization

For probe synthesis, a single coding exon was PCR-amplified from *w¹¹¹⁸* genomic DNA, using a reverse primer with the T7 promoter sequence (see Supplemental Experimental Procedures). The PCR products were purified by Qiaquick gel purification (QIAGEN) and antisense probes synthesized using a DIG RNA labeling kit (Roche). For *trtl* mRNA, we used a probe against *GFP* on tissue expressing the *Trtl-GFP* protein trap. The antisense *GFP* probe was synthesized from the *pBS-eGFP* vector, by linearizing with KpnI and transcribing with the T7 polymerase. Probes were detected using an HRP-conjugated sheep anti-DIG antibody (1:1,000, Roche), followed by TSA Cyanine 3 staining (Perkin Elmer). Ovaries were then stained with mouse anti- α -Spectrin (1:50, DSHB, concentrate). Samples were mounted in SlowFade Antifade (Invitrogen). Images were obtained using a Zeiss LSM 510 confocal microscope and processed with Photoshop.

Immunofluorescence and Staining

Ovaries were dissected in S2 medium and fixed for 15 min in 4% EM-grade formaldehyde (Polysciences). Antibody stains were performed in PBS with 0.1% Triton, and detected using Alexa Fluor-conjugated secondary antibodies (1:200, Invitrogen). TRITC-Phalloidin (1:200, Sigma) or AlexaFluor-647 Phalloidin (1:50, Invitrogen) were used to label cell cortices. ER-Tracker Red (Invitrogen) was diluted in PBS with 4% EM-grade formaldehyde (Polysciences) and the staining reaction was incubated at 37°C for 20 min. Egg chambers were mounted in SlowFade Antifade (Invitrogen) and visualized using a Zeiss LSM 510 confocal microscope. Commercial antibodies include mouse α -KDEL (10C3, 1:25, Calbiochem), rabbit α -GM130 (1:200, Abcam), rabbit α -HA (1:200, Rockland), mouse α -Rab11 (1:20, BD Biosciences), and rabbit α -LanB1 (1:100, Abcam). DSHB antibodies include mouse α -Notch (C458.2H, 1:20), rat α -DE-Cadherin (DCAD2, 1:20), mouse α -FasII (1D4, 1:10), and mouse α -FasIII (7G10, 1:10). Rabbit α -laminin (1:100), rabbit α -Pcan (1:1,000), and rabbit α -nidogen (1:1,000) are from Fessler et al. (1987), Friedrich et al. (2000), and Wolfstetter et al. (2009), respectively. Guinea pig α -Tango1 (1:200) is from this study.

Live Imaging

Live imaging of follicle cell migration was performed as described (Prasad et al., 2007), with the following modifications. Dissected egg chambers were placed onto a pad of 0.4% NuSieve GTG low melt agarose (Lonza) in live imaging medium, and follicle cell membranes were marked with 6.6 μ M FM4-64FX (Invitrogen). The coverslip was cushioned with vacuum grease at each corner, and then sealed with halocarbon oil 27 (Sigma). Confocal movies were taken on a Zeiss LSM 510 microscope, and processed using LSM image browser. TIRF movies were taken on an Olympus IX-50 microscope equipped with an iXon EMCCD camera (Andor) and a 100 \times objective fitted with through-the-objective TIRF illumination, and processed using ImageJ.

SUPPLEMENTAL INFORMATION

Supplemental Information includes seven figures, three movies, and Supplemental Experimental Procedures and can be found with this article online at <http://dx.doi.org/10.1016/j.devcel.2012.12.005>.

ACKNOWLEDGMENTS

Trudi Schüpbach, Lisa Fessler, Stefan Baumgartner, and Anne Holz generously provided reagents. We are grateful to Amanda Neisch for help with antibody production, Pam Vanderzalm for advice on colPs, Guillermina Ramirez-San Juan for MATLAB assistance, and Nick Badovinac for illustrations. We also thank Chip Ferguson, Ben Glick, Lucy O'Brien, and members of the Horne-Badovinac laboratory for comments on the manuscript. This work was supported by National Science Foundation predoctoral fellowships to D.W.L. and A.J.I., as well as a Basil O'Connor Starter Scholar Award (5-FY10-50) from the March of Dimes and NIH grant (R01GM094276) to S.H.-B.

Received: June 26, 2012

Revised: October 16, 2012

Accepted: December 4, 2012

Published: January 28, 2013

REFERENCES

- Amaoutova, I., George, J., Kleinman, H.K., and Benton, G. (2012). Basement membrane matrix (BME) has multiple uses with stem cells. *Stem Cell Rev.* **8**, 163–169.
- Babbey, C.M., Ahktar, N., Wang, E., Chen, C.C., Grant, B.D., and Dunn, K.W. (2006). Rab10 regulates membrane transport through early endosomes of polarized Madin-Darby canine kidney cells. *Mol. Biol. Cell* **17**, 3156–3175.
- Babbey, C.M., Bacallao, R.L., and Dunn, K.W. (2010). Rab10 associates with primary cilia and the exocyst complex in renal epithelial cells. *Am. J. Physiol. Renal Physiol.* **299**, F495–F506.
- Bilder, D., and Haigo, S.L. (2012). Expanding the morphogenetic repertoire: perspectives from the *Drosophila* egg. *Dev. Cell* **22**, 12–23.
- Boll, W., Partin, J.S., Katz, A.I., Caplan, M.J., and Jamieson, J.D. (1991). Distinct pathways for basolateral targeting of membrane and secretory proteins in polarized epithelial cells. *Proc. Natl. Acad. Sci. USA* **88**, 8592–8596.
- Bunt, S., Hooley, C., Hu, N., Scahill, C., Weavers, H., and Skaer, H. (2010). Hemocyte-secreted type IV collagen enhances BMP signaling to guide renal tubule morphogenesis in *Drosophila*. *Dev. Cell* **19**, 296–306.
- Bunt, S., Denholm, B., and Skaer, H. (2011). Characterisation of the *Drosophila* procollagen lysyl hydroxylase, dPlod. *Gene Expr. Patterns* **11**, 72–78.
- Buszczak, M., Paterno, S., Lighthouse, D., Bachman, J., Planck, J., Owen, S., Skora, A.D., Nystul, T.G., Ohlstein, B., Allen, A., et al. (2007). The Carnegie protein trap library: a versatile tool for *Drosophila* developmental studies. *Genetics* **175**, 1505–1531.
- Cao, Z., Li, C., Higginbotham, J.N., Franklin, J.L., Tabb, D.L., Graves-Deal, R., Hill, S., Cheek, K., Jerome, W.G., Lapiere, L.A., et al. (2008). Use of fluorescence-activated vesicle sorting for isolation of Naked2-associated, basolaterally targeted exocytic vesicles for proteomics analysis. *Mol. Cell. Proteomics* **7**, 1651–1667.
- Caplan, M.J., Stow, J.L., Newman, A.P., Madri, J., Anderson, H.C., Farquhar, M.G., Palade, G.E., and Jamieson, J.D. (1987). Dependence on pH of polarized sorting of secreted proteins. *Nature* **329**, 632–635.
- Chen, C.C., Schweinsberg, P.J., Vashist, S., Mareiniss, D.P., Lambie, E.J., and Grant, B.D. (2006). RAB-10 is required for endocytic recycling in the *Caenorhabditis elegans* intestine. *Mol. Biol. Cell* **17**, 1286–1297.
- Chen, Y., Wang, Y., Zhang, J., Deng, Y., Jiang, L., Song, E., Wu, X.S., Hammer, J.A., Xu, T., and Lippincott-Schwartz, J. (2012). Rab10 and myosin-Va mediate insulin-stimulated GLUT4 storage vesicle translocation in adipocytes. *J. Cell Biol.* **198**, 545–560.
- Cohen, D., Müsch, A., and Rodriguez-Boulán, E. (2001). Selective control of basolateral membrane protein polarity by cdc42. *Traffic* **2**, 556–564.
- De Almeida, J.B., and Stow, J.L. (1991). Disruption of microtubules alters polarity of basement membrane proteoglycan secretion in epithelial cells. *Am. J. Physiol.* **261**, C691–C700.
- Denef, N., Chen, Y., Weeks, S.D., Barcelo, G., and Schüpbach, T. (2008). Crag regulates epithelial architecture and polarized deposition of basement membrane proteins in *Drosophila*. *Dev. Cell* **14**, 354–364.
- Eastburn, D.J., and Mostov, K.E. (2010). Laying the foundation for epithelia: insights into polarized basement membrane deposition. *EMBO Rep.* **11**, 329–330.
- Fata, J.E., Werb, Z., and Bissell, M.J. (2004). Regulation of mammary gland branching morphogenesis by the extracellular matrix and its remodeling enzymes. *Breast Cancer Res.* **6**, 1–11.
- Fessler, L.I., Campbell, A.G., Duncan, K.G., and Fessler, J.H. (1987). *Drosophila* laminin: characterization and localization. *J. Cell Biol.* **105**, 2383–2391.
- Friedrich, M.V., Schneider, M., Timpl, R., and Baumgartner, S. (2000). Perlecan domain V of *Drosophila melanogaster*. Sequence, recombinant analysis and tissue expression. *Eur. J. Biochem.* **267**, 3149–3159.
- Fromme, J.C., and Schekman, R. (2005). COPII-coated vesicles: flexible enough for large cargo? *Curr. Opin. Cell Biol.* **17**, 345–352.
- Gutzeit, H.O. (1990). The microfilament pattern in the somatic follicle cells of mid-vitellogenic ovarian follicles of *Drosophila*. *Eur. J. Cell Biol.* **53**, 349–356.
- Gutzeit, H.O., Eberhardt, W., and Gratwohl, E. (1991). Laminin and basement membrane-associated microfilaments in wild-type and mutant *Drosophila* ovarian follicles. *J. Cell Sci.* **100**, 781–788.
- Haigo, S.L., and Bilder, D. (2011). Global tissue revolutions in a morphogenetic movement controlling elongation. *Science* **331**, 1071–1074.
- Herpers, B., and Rabouille, C. (2004). mRNA localization and ER-based protein sorting mechanisms dictate the use of transitional endoplasmic reticulum-golgi units involved in gurken transport in *Drosophila* oocytes. *Mol. Biol. Cell* **15**, 5306–5317.
- Horne-Badovinac, S., and Bilder, D. (2008). Dynein regulates epithelial polarity and the apical localization of stardust A mRNA. *PLoS Genet.* **4**, e8.
- Horne-Badovinac, S., Hill, J., Gerlach, G., 2nd, Menegas, W., and Bilder, D. (2012). A screen for round egg mutants in *Drosophila* identifies tricomered, furry, and misshapen as regulators of egg chamber elongation. *G3 (Bethesda)* **2**, 371–378.
- Hutagalung, A.H., and Novick, P.J. (2011). Role of Rab GTPases in membrane traffic and cell physiology. *Physiol. Rev.* **91**, 119–149.
- Jin, L., Pahuja, K.B., Wickliffe, K.E., Gorur, A., Baumgärtel, C., Schekman, R., and Rape, M. (2012). Ubiquitin-dependent regulation of COPII coat size and function. *Nature* **482**, 495–500.
- Kalluri, R. (2003). Basement membranes: structure, assembly and role in tumour angiogenesis. *Nat. Rev. Cancer* **3**, 422–433.
- Khoshnoodi, J., Pedchenko, V., and Hudson, B.G. (2008). Mammalian collagen IV. *Microsc. Res. Tech.* **71**, 357–370.
- Kondylis, V., and Rabouille, C. (2009). The Golgi apparatus: lessons from *Drosophila*. *FEBS Lett.* **583**, 3827–3838.
- Kondylis, V., Pizette, S., and Rabouille, C. (2009). The early secretory pathway in development: a tale of proteins and mRNAs. *Semin. Cell Dev. Biol.* **20**, 817–827.
- Konopka, C.A., and Bednarek, S.Y. (2008). Variable-angle epifluorescence microscopy: a new way to look at protein dynamics in the plant cell cortex. *Plant J.* **53**, 186–196.
- Konsolaki, M., and Schüpbach, T. (1998). Windbeutel, a gene required for dorsoventral patterning in *Drosophila*, encodes a protein that has homologies to vertebrate proteins of the endoplasmic reticulum. *Genes Dev.* **12**, 120–131.
- Li, G., and Stahl, P.D. (1993). Structure-function relationship of the small GTPase rab5. *J. Biol. Chem.* **268**, 24475–24480.
- Li, Z., Wang, L., Hays, T.S., and Cai, Y. (2008). Dynein-mediated apical localization of crumbs transcripts is required for Crumbs activity in epithelial polarity. *J. Cell Biol.* **180**, 31–38.
- Lu, H., and Bilder, D. (2005). Endocytic control of epithelial polarity and proliferation in *Drosophila*. *Nat. Cell Biol.* **7**, 1232–1239.
- Malhotra, V., and Erlmann, P. (2011). Protein export at the ER: loading big collagens into COPII carriers. *EMBO J.* **30**, 3475–3480.
- Marat, A.L., Dokainish, H., and McPherson, P.S. (2011). DENN domain proteins: regulators of Rab GTPases. *J. Biol. Chem.* **286**, 13791–13800.
- Mellman, I., and Nelson, W.J. (2008). Coordinated protein sorting, targeting and distribution in polarized cells. *Nat. Rev. Mol. Cell Biol.* **9**, 833–845.
- Miner, J.H. (2011). Glomerular basement membrane composition and the filtration barrier. *Pediatr. Nephrol.* **26**, 1413–1417.
- Miner, J.H., and Yurchenco, P.D. (2004). Laminin functions in tissue morphogenesis. *Annu. Rev. Cell Dev. Biol.* **20**, 255–284.
- Mirouse, V., Christoforou, C.P., Fritsch, C., St Johnston, D., and Ray, R.P. (2009). Dystroglycan and perlecan provide a basal cue required for epithelial polarity during energetic stress. *Dev. Cell* **16**, 83–92.
- Mirre, C., Cecchini, J.P., Le Parco, Y., and Knibiehler, B. (1988). De novo expression of a type IV collagen gene in *Drosophila* embryos is restricted to mesodermal derivatives and occurs at germ band shortening. *Development* **102**, 369–376.
- Myllyharju, J., and Kivirikko, K.I. (2004). Collagens, modifying enzymes and their mutations in humans, flies and worms. *Trends Genet.* **20**, 33–43.
- Myllylä, R., Wang, C., Heikkinen, J., Juffer, A., Lampela, O., Risteli, M., Ruotsalainen, H., Salo, A., and Sipilä, L. (2007). Expanding the lysyl

- hydroxylase toolbox: new insights into the localization and activities of lysyl hydroxylase 3 (LH3). *J. Cell. Physiol.* **212**, 323–329.
- Natzle, J.E., Monson, J.M., and McCarthy, B.J. (1982). Cytogenetic location and expression of collagen-like genes in *Drosophila*. *Nature* **296**, 368–371.
- Norman, K.R., and Moerman, D.G. (2000). The *let-268* locus of *Caenorhabditis elegans* encodes a procollagen lysyl hydroxylase that is essential for type IV collagen secretion. *Dev. Biol.* **227**, 690–705.
- O'Brien, L.E., Jou, T.S., Pollack, A.L., Zhang, Q., Hansen, S.H., Yurchenco, P., and Mostov, K.E. (2001). Rac1 orientates epithelial apical polarity through effects on basolateral laminin assembly. *Nat. Cell Biol.* **3**, 831–838.
- Pastor-Pareja, J.C., and Xu, T. (2011). Shaping cells and organs in *Drosophila* by opposing roles of fat body-secreted Collagen IV and perlecan. *Dev. Cell* **21**, 245–256.
- Prasad, M., Jang, A.C., Starz-Gaiano, M., Melani, M., and Montell, D.J. (2007). A protocol for culturing *Drosophila melanogaster* stage 9 egg chambers for live imaging. *Nat. Protoc.* **2**, 2467–2473.
- Ramírez, O.A., and Couve, A. (2011). The endoplasmic reticulum and protein trafficking in dendrites and axons. *Trends Cell Biol.* **21**, 219–227.
- Rautavuoma, K., Takaluoma, K., Sormunen, R., Myllyharju, J., Kivirikko, K.I., and Soininen, R. (2004). Premature aggregation of type IV collagen and early lethality in lysyl hydroxylase 3 null mice. *Proc. Natl. Acad. Sci. USA* **101**, 14120–14125.
- Rodriguez-Boulan, E., Kreitzer, G., and Müsch, A. (2005). Organization of vesicular trafficking in epithelia. *Nat. Rev. Mol. Cell Biol.* **6**, 233–247.
- Saito, K., Chen, M., Bard, F., Chen, S., Zhou, H., Woodley, D., Polischuk, R., Schekman, R., and Malhotra, V. (2009). TANGO1 facilitates cargo loading at endoplasmic reticulum exit sites. *Cell* **136**, 891–902.
- Sano, H., Eguez, L., Teruel, M.N., Fukuda, M., Chuang, T.D., Chavez, J.A., Lienhard, G.E., and McGraw, T.E. (2007). Rab10, a target of the AS160 Rab GAP, is required for insulin-stimulated translocation of GLUT4 to the adipocyte plasma membrane. *Cell Metab.* **5**, 293–303.
- Satoh, A.K., O'Tousa, J.E., Ozaki, K., and Ready, D.F. (2005). Rab11 mediates post-Golgi trafficking of rhodopsin to the photosensitive apical membrane of *Drosophila* photoreceptors. *Development* **132**, 1487–1497.
- Schneider, M., Khailil, A.A., Poulton, J., Castillejo-Lopez, C., Egger-Adam, D., Wodarz, A., Deng, W.M., and Baumgartner, S. (2006). Perlecan and Dystroglycan act at the basal side of the *Drosophila* follicular epithelium to maintain epithelial organization. *Development* **133**, 3805–3815.
- Schneider, V.A., and Granato, M. (2006). The myotomal diwanka (lh3) glycosyltransferase and type XVIII collagen are critical for motor growth cone migration. *Neuron* **50**, 683–695.
- Schuck, S., Gerl, M.J., Ang, A., Manninen, A., Keller, P., Mellman, I., and Simons, K. (2007). Rab10 is involved in basolateral transport in polarized Madin-Darby canine kidney cells. *Traffic* **8**, 47–60.
- Shi, A., Chen, C.C., Banerjee, R., Glodowski, D., Audhya, A., Rongo, C., and Grant, B.D. (2010). EHBP-1 functions with RAB-10 during endocytic recycling in *Caenorhabditis elegans*. *Mol. Biol. Cell* **21**, 2930–2943.
- Simmonds, A.J., dosSantos, G., Livne-Bar, I., and Krause, H.M. (2001). Apical localization of wingless transcripts is required for wingless signaling. *Cell* **105**, 197–207.
- Sipilä, L., Ruotsalainen, H., Sormunen, R., Baker, N.L., Lamandé, S.R., Vapola, M., Wang, C., Sado, Y., Aszodi, A., and Myllylä, R. (2007). Secretion and assembly of type IV and VI collagens depend on glycosylation of hydroxylysines. *J. Biol. Chem.* **282**, 33381–33388.
- Sorrosal, G., Pérez, L., Herranz, H., and Milán, M. (2010). Scarface, a secreted serine protease-like protein, regulates polarized localization of laminin A at the basement membrane of the *Drosophila* embryo. *EMBO Rep.* **11**, 373–379.
- Stenmark, H., Parton, R.G., Steele-Mortimer, O., Lütcke, A., Gruenberg, J., and Zerial, M. (1994). Inhibition of rab5 GTPase activity stimulates membrane fusion in endocytosis. *EMBO J.* **13**, 1287–1296.
- Sütterlin, C., and Colanzi, A. (2010). The Golgi and the centrosome: building a functional partnership. *J. Cell Biol.* **188**, 621–628.
- Tokunaga, M., Imamoto, N., and Sakata-Sogawa, K. (2008). Highly inclined thin illumination enables clear single-molecule imaging in cells. *Nat. Methods* **5**, 159–161.
- Urbano, J.M., Torgler, C.N., Molnar, C., Tepass, U., López-Varea, A., Brown, N.H., de Celis, J.F., and Martín-Bermudo, M.D. (2009). *Drosophila* laminins act as key regulators of basement membrane assembly and morphogenesis. *Development* **136**, 4165–4176.
- Valastyan, S., and Weinberg, R.A. (2011). Tumor metastasis: molecular insights and evolving paradigms. *Cell* **147**, 275–292.
- Venditti, R., Scanu, T., Santoro, M., Di Tullio, G., Spaar, A., Gaibisso, R., Beznoussenko, G.V., Mironov, A.A., Mironov, A., Jr., Zelante, L., et al. (2012). Sedlin controls the ER export of procollagen by regulating the Sar1 cycle. *Science* **337**, 1668–1672.
- Vertel, B.M., Velasco, A., LaFrance, S., Walters, L., and Kaczman-Daniel, K. (1989). Precursors of chondroitin sulfate proteoglycan are segregated within a subcompartment of the chondrocyte endoplasmic reticulum. *J. Cell Biol.* **109**, 1827–1836.
- Viktorinová, I., König, T., Schlichting, K., and Dahmann, C. (2009). The cadherin Fat2 is required for planar cell polarity in the *Drosophila* ovary. *Development* **136**, 4123–4132.
- Wang, T., Liu, Y., Xu, X.H., Deng, C.Y., Wu, K.Y., Zhu, J., Fu, X.Q., He, M., and Luo, Z.G. (2011). Lgl1 activation of rab10 promotes axonal membrane trafficking underlying neuronal polarization. *Dev. Cell* **21**, 431–444.
- Wang, X., Harris, R.E., Bayston, L.J., and Ashe, H.L. (2008). Type IV collagens regulate BMP signalling in *Drosophila*. *Nature* **455**, 72–77.
- Wilson, D.G., Phamluong, K., Li, L., Sun, M., Cao, T.C., Liu, P.S., Modrusan, Z., Sandoval, W.N., Rangell, L., Carano, R.A., et al. (2011). Global defects in collagen secretion in a Mia3/TANGO1 knockout mouse. *J. Cell Biol.* **193**, 935–951.
- Wolfstetter, G., Shirinian, M., Stute, C., Grabbe, C., Hummel, T., Baumgartner, S., Palmer, R.H., and Holz, A. (2009). Fusion of circular and longitudinal muscles in *Drosophila* is independent of the endoderm but further visceral muscle differentiation requires a close contact between mesoderm and endoderm. *Mech. Dev.* **126**, 721–736.
- Xu, J., Lan, L., Bogard, N., Mattione, C., and Cohen, R.S. (2011). Rab11 is required for epithelial cell viability, terminal differentiation, and suppression of tumor-like growth in the *Drosophila* egg chamber. *PLoS ONE* **6**, e20180.
- Yadav, S., and Linstedt, A.D. (2011). Golgi positioning. *Cold Spring Harb. Perspect. Biol.* **3**.
- Yasothornsrikul, S., Davis, W.J., Cramer, G., Kimbrell, D.A., and Dearolf, C.R. (1997). Viking: identification and characterization of a second type IV collagen in *Drosophila*. *Gene* **198**, 17–25.
- Yoshimura, S., Gerondopoulos, A., Linford, A., Rigden, D.J., and Barr, F.A. (2010). Family-wide characterization of the DENN domain Rab GDP-GTP exchange factors. *J. Cell Biol.* **191**, 367–381.
- Yurchenco, P.D. (2011). Basement membranes: cell scaffoldings and signaling platforms. *Cold Spring Harb. Perspect. Biol.* **3**.
- Zhang, J., Schulze, K.L., Hiesinger, P.R., Suyama, K., Wang, S., Fish, M., Acar, M., Hoskins, R.A., Bellen, H.J., and Scott, M.P. (2007). Thirty-one flavors of *Drosophila* rab proteins. *Genetics* **176**, 1307–1322.
- Zhu, H., Zhu, G., Liu, J., Liang, Z., Zhang, X.C., and Li, G. (2007). Rabaptin-5-independent membrane targeting and Rab5 activation by Rabex-5 in the cell. *Mol. Biol. Cell* **18**, 4119–4128.